ORBIT DETERMINATION FOR LUNAR PARKING

ORBITS USING TIME-VARYING ORBITAL ELEMENTS

May 7, 1970

Bellcomm

ORBIT DETERMINATION FOR LUNAR PARKING

ORBITS USING TIME-VARYING ORBITAL ELEMENTS

May 7, 1970

M. V. Bullock
A. J. Ferrari

ABSTRACT

A lunar orbit determination program (Osculating Lunar Elements Program - OLEP) has been developed that represents perturbed vehicle motion by time-varying orbital elements. The program estimates perturbing effects of non-central gravity anomalies, so the concept does not rely on any assumed lunar gravity model.

Doppler tracking data from the lunar orbits of Lunar Orbiter III, Apollo 8, 10, 11, and 12 missions have been processed, and the results are presented. The solutions obtained from these data show OLEP to be effective for use in lunar navigation and orbit prediction. A comparison between OLEP and one current standard technique, shows OLEP propagation errors smaller by a factor of 2.5 or more.

This concept shows potential for application to future Apollo missions and to deep space missions involving planets whose gravity fields are not well known.

TABLE OF CONTENTS

ORBIT DETERMINATION FOR LUNAR PARKING
ORBITS USING TIME-VARYING ORBITAL ELEMENTS

I. INTRODUCTION

        Satellite motion in a central force field is uniquely
specified by six integration constants. Geometrically, these
constants are usually interpreted as the classical Kepler
elements $(a, e, \Omega, \omega, I, T_o)$. For the case of motion in a
non-central gravity field, the Kepler elements become coupled
functions of time.

        Veis and Moore[1] suggested that, for non-central
motion, each of the orbital elements be represented as an in-
dependent time function. This representation has been used in
the Osculating Lunar Elements Program (OLEP), which was
developed for lunar parking orbits. This program provides
estimates for the constant and time-dependent parts of each
element. OLEP determines the perturbing effects of the non-
central field and hence does not rely on any assumed lunar
gravity model.

        Doppler tracking data acquired during the Lunar
Orbiter III and all the lunar Apollo missions have been
processed. Examples of orbit determinations obtained from
these data are presented to illustrate the effectiveness of
OLEP. A comparison is also presented between a conventional
orbit determination program and OLEP.

        This report presents the theory and equations that
constitute OLEP.

II. MATHEMATICAL THEORY

        The long-period time dependence induced in each of
the orbital elements by a non-central gravity field is given
by the Variation of Parameters Equations:[2]

$$\frac{d\bar{s}}{dt} = \bar{f}(\bar{s}, t) \tag{1}$$

where $\bar{s}$ is a six-vector composed of the Kepler orbital state. The equations are a set of six non-linear, coupled, ordinary differential equations. In general, closed form solutions to these equations are not obtainable. Since the non-central effects are extremely small compared to the central body term, solutions to these equations can be sought using perturbation methods.

If an analytic quadrature is performed on each Variation of Parameters Equation, a set of integral equations results:

$$\bar{s}(t) = \bar{s}(t_o) + \int_{t_o}^{t_f} \bar{f}(\bar{s},t)\ dt \qquad (2)$$

The kernels, or forcing functions, appearing in this equation are non-separable, non-linear functions that can be categorized in two types:[3]

1. $\bar{f}(\bar{s},t) = \bar{g}(\bar{s})$ (autonomous)

2. $\bar{f}(\bar{s},t) = \bar{h}(\bar{s})\ \sin m\alpha t + \bar{k}(\bar{s})\ \cos m\alpha t$

$$m=1,2,\ldots$$

where α is the rotational rate of the gravitating body (1/28 rev/day for the moon). The first kernel corresponds to radius- and latitude-dependent perturbations (zonal terms), and the second corresponds to radius-, latitude-, and longitude-dependent perturbations (tesseral and sectorial terms). If it is assumed that for periods of about 24 hours the magnitude of variation in the Kepler elements of a satellite is small, then $\bar{g}(\bar{s})$, $\bar{h}(\bar{s})$, and $\bar{k}(\bar{s})$ can each be assumed constant.

Solutions to equations possessing autonomous kernels have the following simple form:

$$\bar{s}(t) = \bar{s}(t_o) + \bar{g}(t_o)\ (t-t_o) \qquad (3)$$

These solutions have the linear properties of secular variations.

Using the same time approximation made previously, solutions for non-autonomous kernels can be given as follows:

$$\bar{s}(t) = \bar{s}(t_o) + \bar{c}_1(t_o) \sin m\alpha(t-t_o) + \bar{c}_2(t_o) \cos m\alpha(t-t_o) \quad (4)$$

where $\bar{c}_1$, $\bar{c}_2$, and $\bar{c}_3$ are constants.

If the period of time $(t-t_o)$ is smaller than the period of the harmonic perturbing term, then this solution can be expanded in a truncated Taylor Series:

$$\bar{s}(t) = \bar{s}(t_o) + \bar{c}_1(t_o) \left[m\alpha(t-t_o) + .. \right] + \bar{c}_2(t_o) \left[1 - \frac{m^2\alpha^2}{2}(t-t_o)^2 + ... \right]$$

$$(5)$$

or $\quad \bar{s}(t) = \bar{\Delta}_o + \bar{\Delta}_1 t + \bar{\Delta}_2 t^2 + \bar{\Delta}_3 t^3 + ...$

where $\bar{\Delta}_o$, $\bar{\Delta}_1$, $\bar{\Delta}_2$, etc. are constants. For the time periods under consideration, OLEP has been configured so that eighteen such series terms can be estimated. Classical short-period variations are not modeled by the solutions given in equations (3) and (5).

Two typical osculating elements (for example, $\Omega(t)$ and $e(t)$) can be represented by the following functional forms:

$$\Omega(t) = \Omega_o + \Omega_1 t \qquad \text{(secular variation)}$$

$$(6)$$

$$e(t) = e_o + e_1 t + e_2 t^2 + e_3 t^3 \quad \text{(secular and long-period variation)}.$$

The terms Ω_o, Ω_1, e_o, e_1, e_2, and e_3 are examples of solution parameters that can be estimated during the orbit determination. The perturbing effects of the sun and earth are implicit in the estimates of the time-varying parameters.

III. DOPPLER OBSERVABLE MODEL

Earth-based angle, range, and Doppler measurements are taken during lunar parking orbits. At lunar distances, the instrumentation limitations associated with angle measurements and ephemeris errors associated with range data make both of these data types less useful than Doppler. OLEP has been structured to model and reduce only Doppler data.

The Doppler observation ($\hat{\lambda}$) is a scalar quantity that is a function of the selenocentric vehicle state, the relative earth/moon configuration and the tracking station position and rotational velocity. During the orbit determination only estimates of the vehicle state are refined.

The vehicle state in lunar orbit is defined using low-eccentricity orbital elements (a, $e_c = e \cos \omega$, $e_s = e \sin \omega$, Ω, I, $m = M + \omega$). This element set eliminates the singularity associated with nearly circular orbits. The indeterminacy associated with equatorial orbits is removed by defining the low-eccentricity elements in a special selenocentric coordinate system ($\bar{Z}$) which represents any orbit as a near-polar orbit. This transformation is accomplished by rotating the initial estimate ($\hat{\bar{X}}$, $\dot{\hat{\bar{X}}}$) of selenocentric state at epoch through two of its associated Euler angles ($\hat{\Omega}$, $\hat{I}$).

$$\bar{Z} = [M] \ \bar{X}$$

$$\dot{\bar{Z}} = [M] \ \dot{\bar{X}}$$

(7)

where

$$M = \begin{bmatrix} \cos \hat{\Omega} & \sin \hat{\Omega} & 0 \\ \sin \hat{\Omega} \sin \hat{I} & -\cos \hat{\Omega} \sin \hat{I} & \cos \hat{I} \\ \sin \hat{\Omega} \cos \hat{I} & -\cos \hat{\Omega} \cos \hat{I} & -\sin \hat{I} \end{bmatrix}$$

Since the original estimates for $\hat{\Omega}$ and $\hat{I}$ are assumed near their converged values, this transformation is performed only once prior to the data reduction.

The semi-major axis does not appear as an explicit solution parameter in OLEP. The estimate for the linear portion of the $(M + \omega)$ angle, $m(t) = m_o + m_1 t$, is used to imply a corresponding semi-major axis (Kepler's third law):

$$a = \left[\frac{\mu}{m_1^2} \right]^{1/3} \tag{8}$$

The orbital state of the vehicle at time t_i is found by evaluating the element functions. This orbital state is converted to the special selenocentric state, $\bar{Z}$ and $\dot{\bar{Z}}$, using the classical equations[4] (Appendix I). The special selenocentric state is transformed into the selenocentric state as follows:

$$\bar{X} = [M]^{-1} \bar{Z}$$

$$\tag{9}$$

$$\dot{\bar{X}} = [M]^{-1} \dot{\bar{Z}}$$

The vehicle state in selenocentric coordinates is translated to earth-centered inertial coordinates, $\bar{Y}$, in the following manner: ($\bar{X}$, $\dot{\bar{X}}$, $\bar{X}_e$, and $\dot{\bar{X}}_e$ have been corrected to account for speed of light delay.)

$$\bar{Y} = \bar{X} + \bar{X}_e - \bar{Y}_s$$

$$\tag{10}$$

$$\dot{\bar{Y}} = \dot{\bar{X}} + \dot{\bar{X}}_e - \dot{\bar{Y}}_s$$

where $\bar{X}_e$ and $\dot{X}_e$ are the position and velocity of the moon's center with respect to that of the earth, $\bar{Y}_s$ and $\dot{Y}_s$ are the geocentric position and velocity of the earth-based tracker. The estimated observable, $\hat{\lambda}$, is expressed in terms of the earth-centered vehicle state[5] (Appendix II):

$$\hat{\lambda} = \hat{\lambda} \; (\bar{Y}, \; \dot{Y}) \tag{11}$$

At any time t_i, the estimated observable $\hat{\lambda}(t_i)$ can be formulated without an assumed lunar gravity field or integrated equations of motion.

IV. LEAST SQUARES ALGORITHM

Orbit determination and estimation are accomplished using a weighted least squares algorithm. This technique minimizes the error squared or residual obtained from processing k observations by differentially correcting n solution parameters $\{\alpha_j\}$ as follows:

$$\Delta\alpha = \left[\sum_{i=1}^{k} J^T(t_i) \; W(t_i) \; J(t_i) \right]^{-1} \sum_{i=1}^{k} J^T(t_i) \; W(t_i) \; \Delta\lambda(t_i) \tag{12}$$

where $\Delta\lambda(t_i) = \lambda(t_i) - \hat{\lambda}(t_i)$

In this expression $\Delta\alpha$ is the differential correction vector (n x 1), $J(t_i)$ is a row vector (1 x n) containing the partial derivatives of the observable with respect to the parameters being estimated (evaluated at time t_i), J^T is the transpose of the J vector, $W(t_i)$ is the reciprocal variance of the observable (assumed constant), $\lambda(t_i)$ is the observation at t_i, and $\hat{\lambda}(t_i)$ is the estimated observable at time t_i.

A typical entry to the J vector (consider the case of $\Omega(t) = \Omega_o + \Omega_1 t$) is found using the chain rule for differentiable functions:

$$\left.\frac{\partial \hat{\lambda}}{\partial \Omega_1}\right|_{t_k} = \left[\sum_{i=1}^{3} \sum_{j=1}^{3} \frac{\partial \hat{\lambda}}{\partial X_i} \frac{\partial X_i}{\partial Z_j} \frac{\partial Z_j}{\partial \Omega} \frac{\partial \Omega}{\partial \Omega_1} + \frac{\partial \hat{\lambda}}{\partial \dot{X}_i} \frac{\partial \dot{X}_i}{\partial \dot{Z}_j} \frac{\partial \dot{Z}_j}{\partial \Omega} \frac{\partial \Omega}{\partial \Omega_1}\right]_{t_k} \quad (13)$$

In this expression $\frac{\partial \hat{\lambda}}{\partial X_i}$ and $\frac{\partial \hat{\lambda}}{\partial \dot{X}_i}$ are the partial derivatives of the observable with respect to the selenocentric state, $\frac{\partial X_i}{\partial Z_j}$ and $\frac{\partial \dot{X}_i}{\partial \dot{Z}_j}$ are partial derivatives (the M^{-1} matrix) of the selenocentric state with respect to the special selenocentric state, $\frac{\partial Z_j}{\partial \Omega}$ and $\frac{\partial \dot{Z}_j}{\partial \Omega}$ are partial derivatives of the special selenocentric state with respect to the orbital element in question (longitude of the ascending node in this case), and $\frac{\partial \Omega}{\partial \Omega_1}$ is the partial derivative of the orbital element with respect to the parameter to be estimated. Each partial derivative appearing in Equation (13) is evaluated at every time t_k over the data interval. All partial derivatives used in Equation (13) are analytically obtained and are given in Appendix III.

The equation representing the differential correction scheme, Equation 12, is a linearization of a non-linear equation and consequently must be solved iteratively. The processing of k observations and the resulting set of differential corrections, $\{\Delta \alpha_j\}$, constitute one computing iteration. The convergence criterion for two successive iterations is as follows:

$$\frac{\left.\sum_{i=1}^{k} [\Delta \lambda(t_i)]^2\right|_{(K-1)}}{\left.\sum_{i=1}^{k} [\Delta \lambda(t_i)]^2\right|_{(K)}} - 1 < \delta \quad (14)$$

where δ is a small positive number (10^{-4}) and (K-1) and (K) designate the (K-1) and (K) computing iterations.

V.   DATA ANALYSIS

Various tests were made to determine the optimum data span to use for OLEP solutions. The results attained by fitting one front side pass of data fulfilled the residual minimization criterion but possessed poor prediction capabilities. An analysis of correlations among solution parameters of a one-pass solution indicated that insufficient orbital period and time-varying information was contained in this data span. Results showed that an optimum solution, in terms both of fit and prediction, can only be attained when two or more passes of data are used. This seems to be the chief limitation of the method.

Data from four lunar orbits, Lunar Orbiter III, Apollo 10, 11, and 12 were selected to demonstrate the fit and prediction capabilities of OLEP. (Data analysis from the Apollo 8 mission is not presented. The vehicle was venting propulsively for almost all the tracking passes, so the data are not representative of free flight.) In each case presented, the solution was obtained by fitting two consecutive front side passes of data. The propagation quality of each solution was assessed by predicting the Doppler for the next two consecutive passes of data. The parameter set used for Lunar Orbiter III, Apollo 10 and 12 data consists of the following terms:

$$\{e_{so},\ e_{s1},\ e_{co},\ e_{c1},\ \Omega_o,\ \Omega_1,\ I_o,\ m_o,\ m_1\}$$

For the case of Apollo 11 data, Ω_1 was deleted from the parameter set since it became highly correlated with other terms. In all cases the addition of the linear inclination term, I_1, led to growth in the Doppler residuals. This condition reflects an insensitivity in the data to this parameter. Quadratic and higher order terms were not included in the solution set since, for the time periods involved (approximately 8 hours), secular and long-period variations are almost identical. The errors associated with each two-pass fit/two-pass propagation are shown in Figures 1 and 2. In each case the residuals manifested no growth between fit and prediction intervals. These errors are systematic and contain a harmonic with an amplitude of 0.8 fps

peak-to-peak and a period about one-fourth the orbital period. These intra-period residuals are characteristic of short-period variations not modeled in OLEP.

In order to evaluate OLEP further, orbit determinations were performed using longer data intervals. Two ten-pass tracking intervals were used, one from Apollo 11 and one from Apollo 12. Experimental analysis showed, for both Apollo 11 and 12 data, that the secular and long-period variations in the orbital elements were best represented by a solution set containing the following twelve parameters:

$$\{e_{s0},\ e_{s1},\ e_{s2},\ e_{c0},\ e_{c1},\ \dot{e}_{c2},\ \Omega_0,\ \dot{\Omega}_1,\ I_0,\ m_0,\ m_1,\ m_2\}$$

The linear inclination term was again excluded from the solution set since it became highly correlated with the orbital motion term, m_1. Doppler errors associated with these longer solutions (see Figure 3) exhibit the same short-period variations and are about the same amplitude as those of the two pass solutions.

VI. COMPARISON WITH STANDARD METHODS

The lunar orbit determination program used by Mission Control Center (MCC) during the Apollo missions is also a weighted least squares estimator. In it, the vehicle dynamics are modeled using integrated rectangular equations of motion based on an assumed lunar gravity field. Presently, the L-1 field is considered best and comparisons between OLEP results and MCC results are of interest. The L-1 orbit determinations were performed using one pass of tracking data, since MCC analysis has shown this is the optimum data interval for use with this method.[6] Doppler residuals from two different L-1 one pass fits and the associated two pass predictions are shown in Figure 4. These residuals are also systematic: a comparison between OLEP and L-1 two pass predictions shows the L-1 errors are about 2.5 times larger in magnitude (peak-to-peak).

Both with OLEP and with conventional programs, the weighted least squares process used contains the effect of the incomplete mathematical representation for the lunar field.

One cannot judge quality of orbit determination only on
smallness of residuals in the fit zone: the incompleteness
of the mathematical models makes it mandatory also to judge
the ability to propagate.

VII. SUMMARY AND CONCLUSIONS

        An orbit determination program has been developed
for lunar orbits. The orbital state of the vehicle is repre-
sented by time-varying functions. This program estimates the
effects of non-central gravity anomalies without relying on
an assumed gravity model or integrated equations of motion.

        Doppler tracking data from the Lunar Orbiter III,
Apollo 10, 11 and 12 missions have been processed, and results
are presented to demonstrate the OLEP concept. Solutions were
obtained by fitting tracking data from the lunar front side of
two consecutive revolutions. Doppler errors (0.8 fps peak-
to-peak) did not grow when each of these solutions was extrapo-
lated into the next two passes of data. Solutions obtained
using ten passes of data have almost identical error distribu-
tions as those of the two-pass solutions. Both the fit and
prediction qualities of OLEP solutions indicate that the approxi-
mations used are a good representation of the non-central pertur-
bations experienced in lunar orbit. A comparison between L-1
and OLEP two pass predictions shows the L-1 Doppler errors
are about 2.5 times larger.

        The overall results of processing tracking data show
OLEP to be effective for lunar navigation and orbit prediction.
This concept shows potential for application to later Apollo
missions and to deep space missions involving planets of unknown
gravity fields.

M. V. Bullock

M. V. Bullock

A. J. Ferrari

2014-$\frac{MVB}{AJF}$-ksc   A. J. Ferrari

BELLCOMM, INC.

The rectangular state components $(\bar{Z}, \dot{\bar{Z}})$ can be obtained from the low-eccentricity elements by first finding the corresponding Kepler elements:

$$e = \sqrt{e_c^2 + e_s^2}$$

$$\omega = \tan^{-1} \frac{e_s}{e_c}$$

$$M = m - \omega$$

and $\quad E - e \sin E = M$

Knowing the standard Kepler elements $(a, e, i, \Omega, \omega, E)$, the rectangular state components are then given as follows:

$$\bar{Z} = [R] \; \bar{q}$$

where the entries to the R matrix are:

$$r_{11} = \cos \Omega \cos \omega - \sin \Omega \cos I \sin \omega$$

$$r_{12} = -\cos \Omega \sin \omega - \sin \Omega \cos I \cos \omega$$

$$r_{13} = \sin \Omega \sin I$$

$$r_{21} = \sin \Omega \cos \omega + \cos \Omega \cos I \sin \omega$$

$$r_{22} = -\sin \Omega \sin \omega + \cos \Omega \cos I \cos \omega$$

$$r_{23} = -\cos \Omega \sin I$$

$$r_{31} = \sin I \sin \omega$$

$$r_{32} = \sin I \cos \omega$$

$$r_{33} = \cos I$$

and:

$$\bar{q} = \begin{bmatrix} a(\cos E - e) \\ a\sqrt{1-e^2} \sin E \\ 0 \end{bmatrix}$$

For the velocity:

$$\dot{\bar{Z}} = \frac{\partial \bar{Z}}{\partial e_s} \dot{e}_s + \frac{\partial \bar{Z}}{\partial e_c} \dot{e}_c + \frac{\partial \bar{Z}}{\partial \Omega} \dot{\Omega} + \frac{\partial \bar{Z}}{\partial I} \dot{I} + \frac{\partial \bar{Z}}{\partial m} \dot{m}$$

The derivatives $\frac{\partial \bar{Z}}{\partial e_s}$, $\frac{\partial \bar{Z}}{\partial e_c}$, $\frac{\partial \bar{Z}}{\partial \Omega}$, $\frac{\partial \bar{Z}}{\partial I}$, and $\frac{\partial \bar{Z}}{\partial m}$ are given in Appendix III. The terms $\dot{e}_s$, $\dot{e}_c$, $\dot{\Omega}$, $\dot{I}$, and $\dot{m}$ are analytically obtainable from the parameter set being used.

BELLCOMM, INC.

APPENDIX II

The estimated Doppler observable, $\hat{\lambda}$, can be computed over some counting interval, τ seconds, using the following set of range equations:

$$\bar{\rho}_4 = \bar{Y}\left(t_r - \frac{\rho_4}{c}\right) - \bar{Y}_{sr}\ (t_r)$$

$$\bar{\rho}_3 = \bar{Y}\left(t_r - \frac{\rho_4}{c}\right) - \bar{Y}_{st}\left[t_r - \left(\frac{\rho_4 + \rho_3}{c}\right)\right]$$

$$\bar{\rho}_2 = \bar{Y}\left(t_r - \tau - \frac{\rho_2}{c}\right) - \bar{Y}_{sr}\ (t_r - \tau)$$

$$\bar{\rho}_1 = \bar{Y}\left(t_r - \tau - \frac{\rho_2}{c}\right) - \bar{Y}_{st}\left[t_r - \tau - \left(\frac{\rho_1 + \rho_2}{c}\right)\right]$$

where $\bar{\rho}_1$, $\bar{\rho}_2$, $\bar{\rho}_3$, and $\bar{\rho}_4$ are ranges expressed in geocentric coordinates, $\bar{Y}$ is the vehicle position, $\bar{Y}_{sr}$ and $\bar{Y}_{st}$ are the receiving and transmitting station positions, t_r is the Doppler time (at the end of the counting interval) and is the time the signal is received at the receiving station, c is the speed of light, and τ is the counting interval (see Figure 1A).

The equations for the four ranges can be solved in an iterative manner. The estimated observable can then be found as follows:

$$\hat{\lambda} = \frac{1}{2\tau}\left[\left(\rho_3 + \rho_4\right) - \left(\rho_1 + \rho_2\right)\right]$$

where $\hat{\lambda}$ is expressed in units of length per time. This value of $\hat{\lambda}$ is valid at $t = t_r - \frac{\tau}{2} - \frac{\rho_4}{c}$.

BELLCOMM, INC.

<div align="center">

APPENDIX III
</div>

I. PARTIAL DERIVATIVES OF THE OBSERVABLE WITH RESPECT TO SELENOCENTRIC STATE

The partial derivatives of the observable (in fps) with respect to the selenocentric position and velocity are used as the following approximate forms:[5]

$$\frac{\partial \hat{\lambda}}{\partial \bar{X}} = \frac{1}{2} \left[\frac{\dot{\rho}_3}{\rho_3} - \frac{\dot{\rho}_3}{\rho_3^2} \bar{\rho}_3 + \frac{\dot{\rho}_4}{\rho_4} - \frac{\dot{\rho}_4}{\rho_4^2} \bar{\rho}_4 \right]$$

$$\frac{\partial \hat{\lambda}}{\partial \dot{\bar{X}}} = \frac{1}{2} \left[\frac{\bar{\rho}_3}{\rho_3} + \frac{\bar{\rho}_4}{\rho_4} \right]$$

In these equations:

$$\bar{\rho}_4 = \bar{X} \left(t_r - \frac{\tau}{2} - \frac{\rho_4}{c} \right) - \bar{X}_{sr} \left(t_r - \frac{\tau}{2} \right)$$

$$\dot{\bar{\rho}}_4 = \dot{\bar{X}} \left(t_r - \frac{\tau}{2} - \frac{\rho_4}{c} \right) - \dot{\bar{X}}_{sr} \left(t_r - \frac{\tau}{2} \right)$$

$$\bar{\rho}_3 = \bar{X} \left(t_r - \frac{\tau}{2} - \frac{\rho_4}{c} \right) - \bar{X}_{st} \left[t_r - \frac{\tau}{2} - \frac{(\rho_3 + \rho_4)}{2} \right]$$

$$\dot{\bar{\rho}}_3 = \dot{\bar{X}} \left(t_r - \frac{\tau}{2} - \frac{\rho_4}{c} \right) - \dot{\bar{X}}_{st} \left[t_r - \frac{\tau}{2} - \frac{(\rho_3 + \rho_4)}{2} \right]$$

and: $\rho_i = |\bar{\rho}_i|$

$$\frac{d\rho_i}{dt} = \frac{\bar{\rho}_i \cdot \dot{\bar{\rho}}_i}{\rho_i}$$

These equations are valid for the time,

$$t = t_r - \frac{\tau}{2} - \frac{\rho_4}{c}$$

II. PARTIAL DERIVATIVES OF THE SELENOCENTRIC STATE WITH RESPECT TO THE SPECIAL SELENOCENTRIC STATE

The partial derivatives of the selenocentric state $(\bar{X}, \dot{\bar{X}})$ with respect to the special selenocentric state $(\bar{Z}, \dot{\bar{Z}})$ are as follows:

$$\frac{\partial X_1}{\partial Z_1} = \cos \hat{\Omega}$$

$$\frac{\partial X_1}{\partial Z_2} = \sin \hat{\Omega} \cos \hat{I}$$

$$\frac{\partial X_1}{\partial Z_3} = \sin \hat{\Omega} \cos \hat{I}$$

$$\frac{\partial X_2}{\partial Z_1} = \sin \hat{\Omega}$$

$$\frac{\partial X_2}{\partial Z_2} = -\cos \hat{\Omega} \sin \hat{I}$$

$$\frac{\partial X_2}{\partial Z_3} = -\cos \hat{\Omega} \cos \hat{I}$$

$$\frac{\partial X_3}{\partial Z_1} = 0$$

$$\frac{\partial X_3}{\partial Z_2} = \cos \hat{I}$$

$$\frac{\partial X_3}{\partial Z_3} = -\sin \hat{I}$$

The transformation $\frac{\partial \dot{\bar{X}}}{\partial \dot{\bar{Z}}}$ is identical to that of the position components above.

III. THE PARTIAL DERIVATIVES OF THE SPECIAL SELENOCENTRIC STATE WITH RESPECT TO THE LOW ECCENTRICITY ELEMENTS

The partial derivatives of the special selenocentric state $(\bar{Z}, \dot{\bar{Z}})$ with respect to the low eccentricity elements $\{a, e_s, e_c, I, \Omega, m\}$ are as follows:

$$\frac{\partial \bar{Z}}{\partial a} = \frac{\bar{Z}}{a}$$

$$\frac{\partial \bar{Z}}{\partial e_s} = \frac{-1}{1-e^2} \left[\sin \phi + e_s - \frac{e_c\, e_{sE}}{1 + \sqrt{1-e^2}} \right] \bar{Z}$$

$$+ \frac{1}{n} \left[-\left(1 + \frac{z}{p}\right) \cos \phi + \frac{z}{p} \frac{e_c\left(e_{cE} + \sqrt{1-e^2}\right)}{1 + \sqrt{1-e^2}} \right] \dot{\bar{Z}}$$

where: $n = \sqrt{\frac{\mu}{a^3}}$, $p = a(1-e^2)$, $\phi = \omega + E$, $e_{sE} = e \sin E$, and $e_{cE} = e \cos E$

$$\frac{\partial \bar{Z}}{\partial e_c} = \frac{-1}{1-e^2} \left[\cos \phi + e_c + \frac{e_s\, e_{sE}}{1 + \sqrt{1-e^2}} \right] \bar{Z}$$

$$+ \frac{1}{n} \left[\left(1 + \frac{z}{p}\right) \sin \phi - \frac{z}{p} e_s \frac{\left(e_{cE} + \sqrt{1-e^2}\right)}{1 + \sqrt{1-e^2}} \right] \dot{\bar{Z}}$$

$$\frac{\partial \bar{Z}}{\partial i} = \begin{bmatrix} Z_3 \sin \Omega \\ -Z_3 \cos \Omega \\ Z_2 \cos \Omega - Z_1 \sin \Omega \end{bmatrix}$$

$$\frac{\partial \bar{Z}}{\partial \Omega} = \begin{bmatrix} -Z_2 \\ Z_1 \\ 0 \end{bmatrix}$$

$$\frac{\partial \bar{Z}}{\partial m} = \frac{1}{n} \dot{\bar{z}}$$

$$\frac{\partial \dot{\bar{Z}}}{\partial a} = -\frac{1}{2} \frac{\dot{\bar{z}}}{a}$$

$$\frac{\partial \dot{\bar{Z}}}{\partial e_s} = \frac{n}{1 - e^2} \left(\frac{a}{Z}\right)^2 \left[\left(\frac{p}{Z} + e_{cE}\right) \cos \phi - e_c \frac{\left(e_{cE}^2 + \sqrt{1 - e^2}\right)}{1 + \sqrt{1 - e^2}}\right] \bar{z}$$

$$+ \frac{1}{1 - e^2} \left(\sin \phi - \frac{e_c e_{sE}}{1 + \sqrt{1 - e^2}}\right) \dot{\bar{z}}$$

$$\frac{\partial \dot{\bar{Z}}}{\partial e_c} = \frac{n}{1 - e^2} \left(\frac{a}{Z}\right)^2 \left[-\left(\frac{p}{Z} + e_{cE}\right) \sin \phi + e_s \frac{\left(e_{cE}^2 + \sqrt{1 - e^2}\right)}{1 + \sqrt{1 - e^2}}\right] \bar{z}$$

$$+ \frac{1}{1 - e^2} \left(\cos \phi + \frac{e_s e_{sE}}{1 + \sqrt{1 - e^2}}\right) \dot{\bar{z}}$$

$$\frac{\partial \dot{\bar{Z}}}{\partial i} = \begin{bmatrix} \dot{z}_3 \sin \Omega \\ -\dot{z}_3 \cos \Omega \\ \dot{z}_2 \cos \Omega - \dot{z}_1 \sin \Omega \end{bmatrix}$$

$$\frac{\partial \dot{Z}}{\partial \Omega} = \begin{bmatrix} -\dot{Z}_2 \\ \\ \dot{Z}_1 \\ \\ 0 \end{bmatrix}$$

$$\frac{\partial \dot{Z}}{\partial m} = -n \left(\frac{a}{Z}\right)^3 \bar{Z}$$

IV. PARTIAL DERIVATIVES OF THE LOW-ECCENTRICITY ELEMENTS WITH RESPECT TO THE PARAMETERS

For the case of a low-eccentricity element, s_k, which is represented by a constant, linear or quadratic function (e.g.)

$$s_k(t) = s_{k0} + s_{k1} t + s_{k2} t^2$$

The required partial derivatives are:

$$\frac{\partial s_k(t)}{\partial s_{k0}} = 1$$

$$\frac{\partial s_k(t)}{\partial s_{k1}} = t$$

$$\frac{\partial s_k(t)}{\partial s_{k2}} = t^2$$

BELLCOMM, INC.

REFERENCES

1. Veis, G., and Moore, C. H., "Smithsonian Astrophysical
    Observatory Differential Orbit Improvement Program",
    Jet Propulsion Laboratory Semiannual Proceedings, Pasadena,
    California, 1960, pp. 161-184.

2. Kaula, W. M., Theory of Satellite Geodesy, Waltham,
    Massachusetts, Blaisdell Publishing Co., 1966, p. 29.

3. Pollard, H., Mathematical Introduction to Celestial
    Mechanics, Englewood Cliffs, New Jersey, 1966, pp. 89-92.

4. Kaula, W. M., Theory of Satellite Geodesy, Waltham,
    Massachusetts, Blaisdell Publishing Co., 1966, pp. 23-24.

5. de Vezin, H. G., "Doppler Observable Modeling for the
    Apollo Real-Time Orbit Determination Program",
    Astrodynamics Conference, December 12-14, 1967, Volume II,
    Orbit Determination Session, NASA MSC Internal Note
    No. 68-FM-136, pp. 43-46.

6. Wollenhaupt, W. R., "Apollo Orbit Determination and
    Navigation", AIAA 8th Aerospace Science Meeting,
    New York, New York, January 19-21, 1970, AIAA Paper
    No. 70-27.
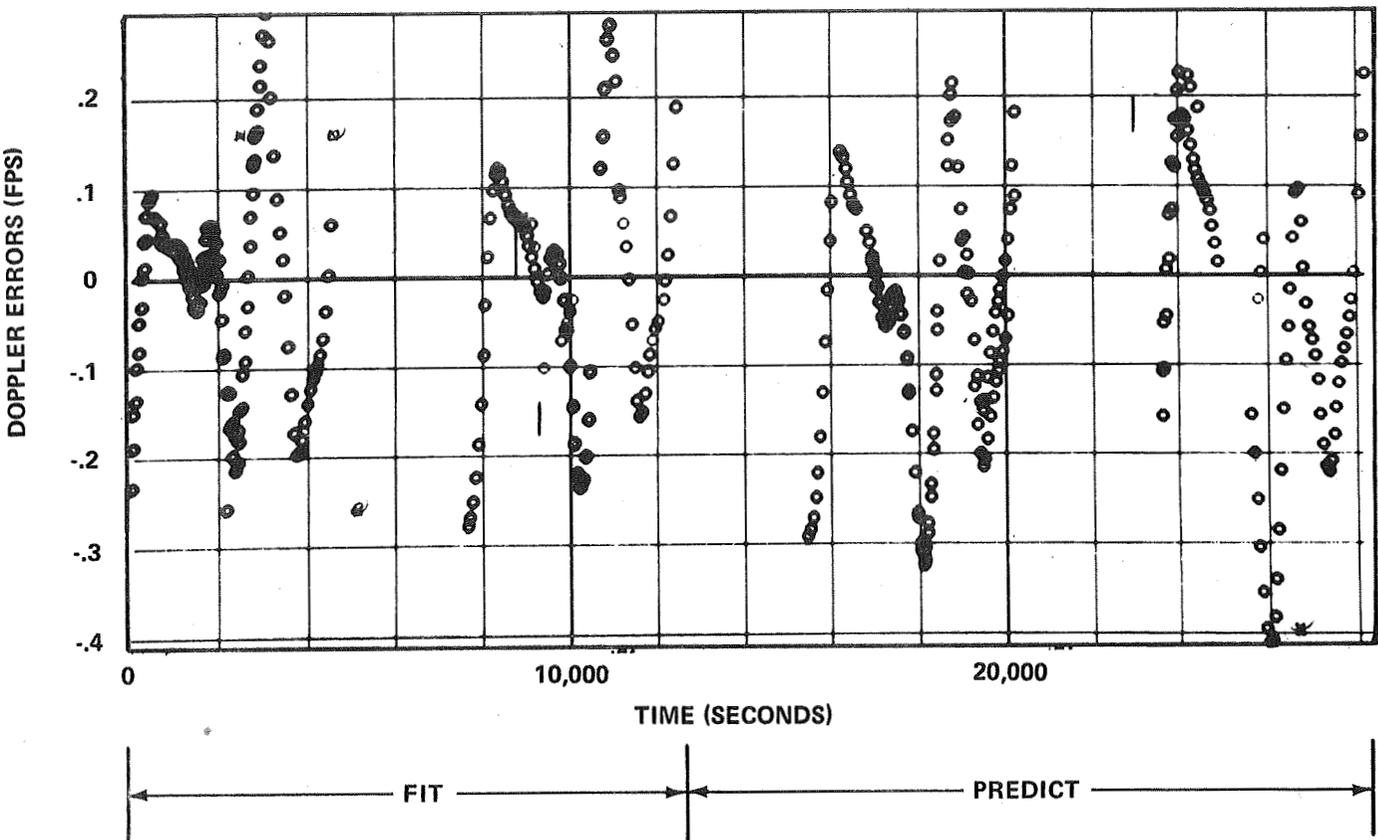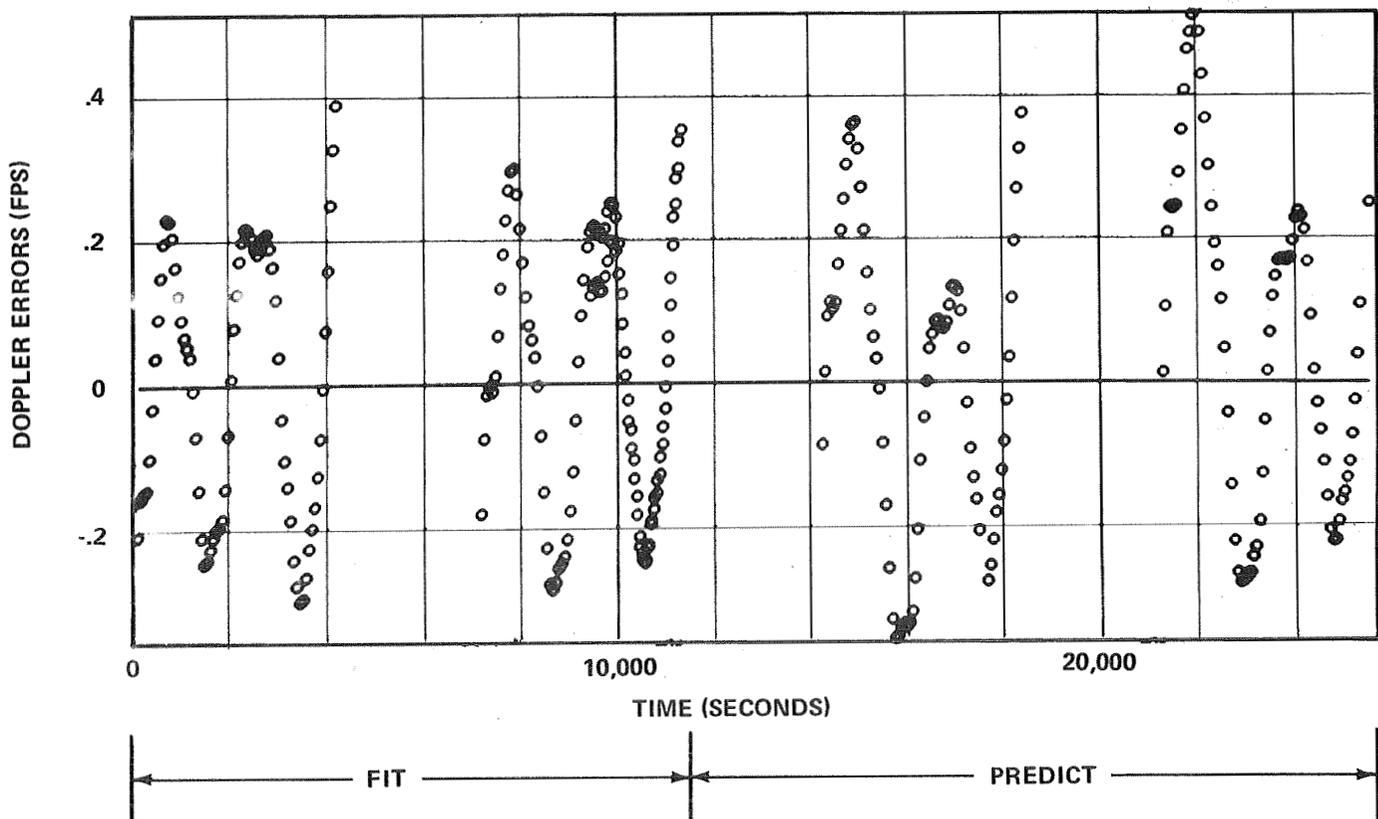
FIGURE 1 - DOPPLER RESIDUALS FROM TWO PASS SOLUTIONS AND PREDICTIONS
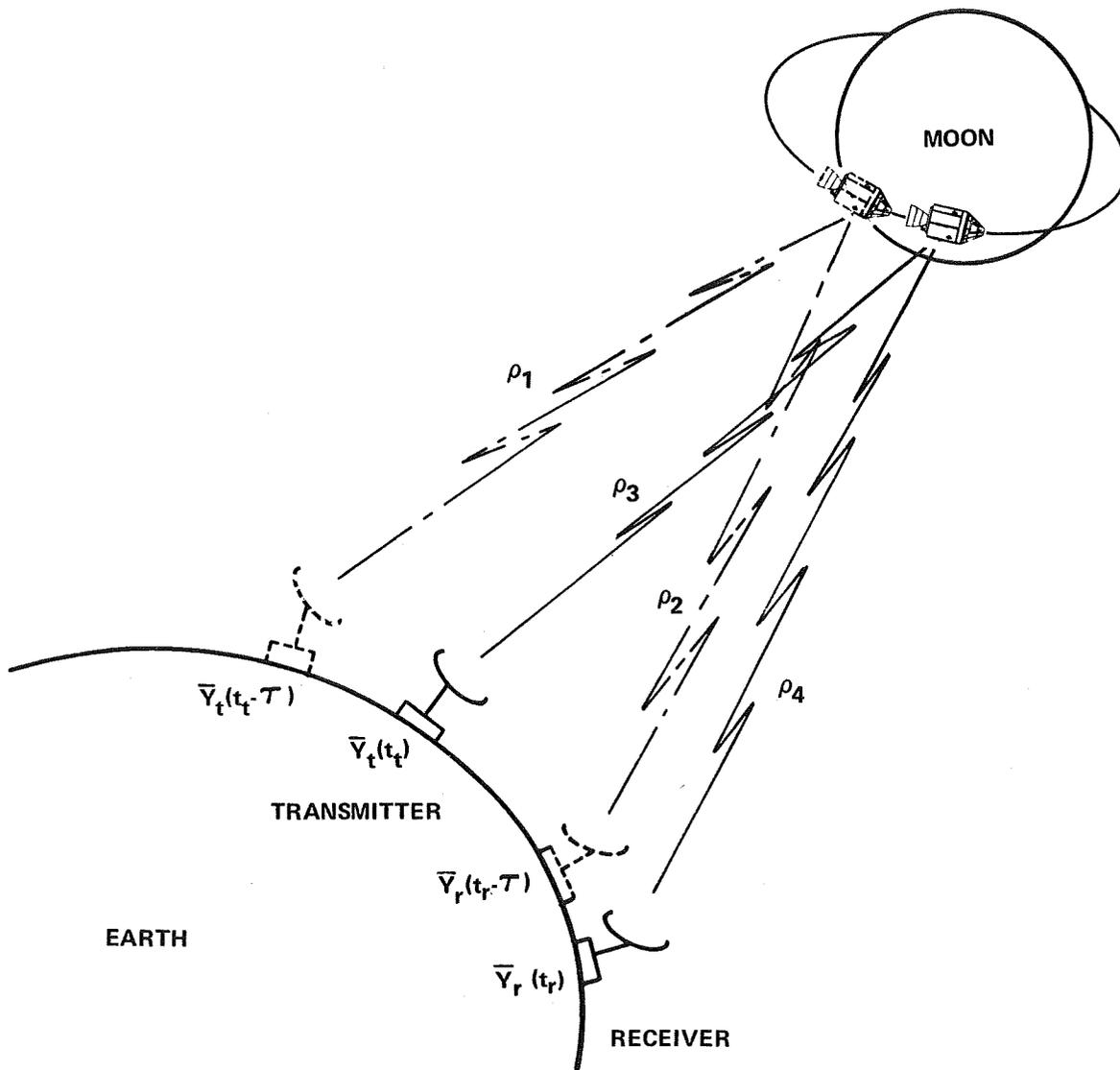
FIGURE 1A - TRACKING GEOMETRY
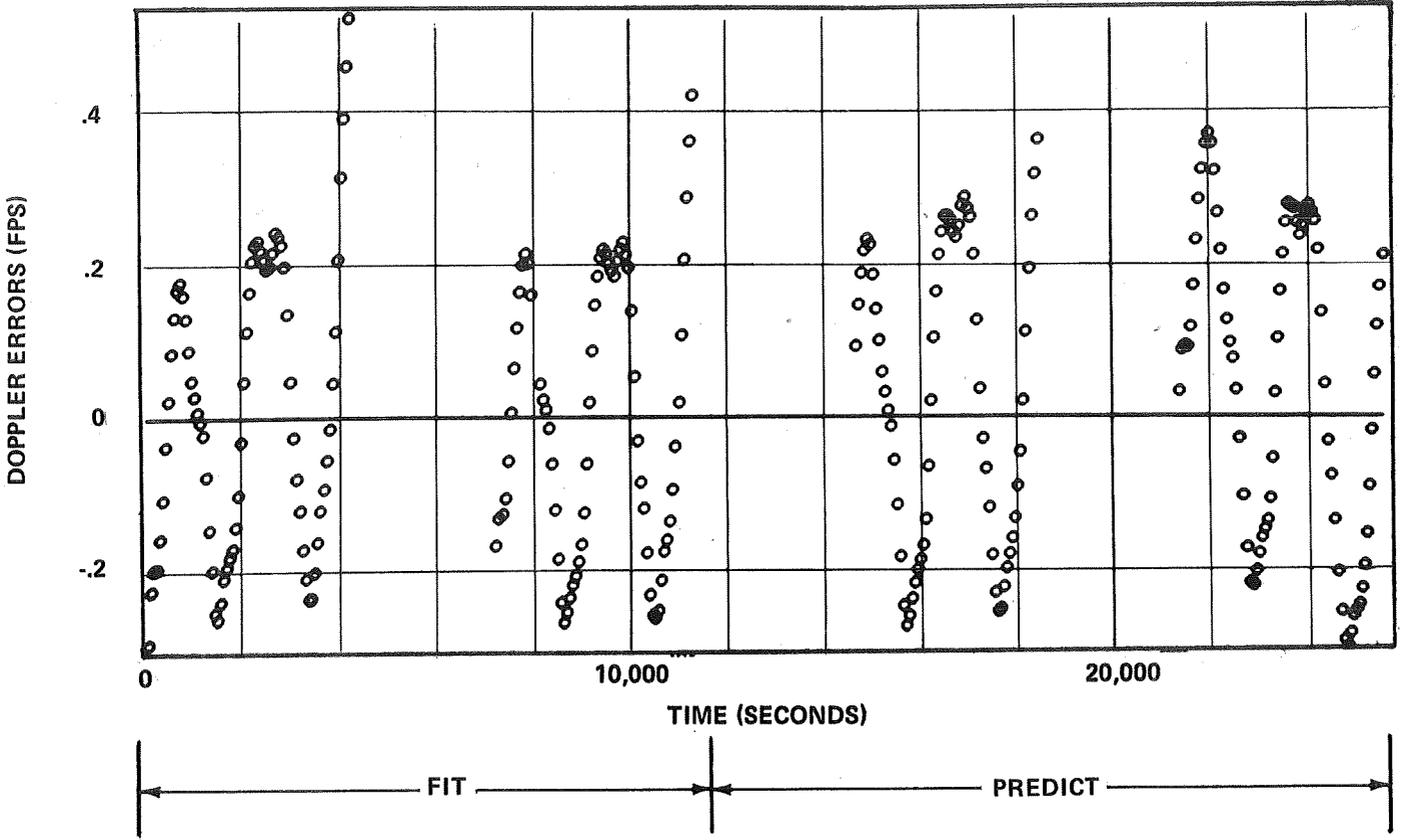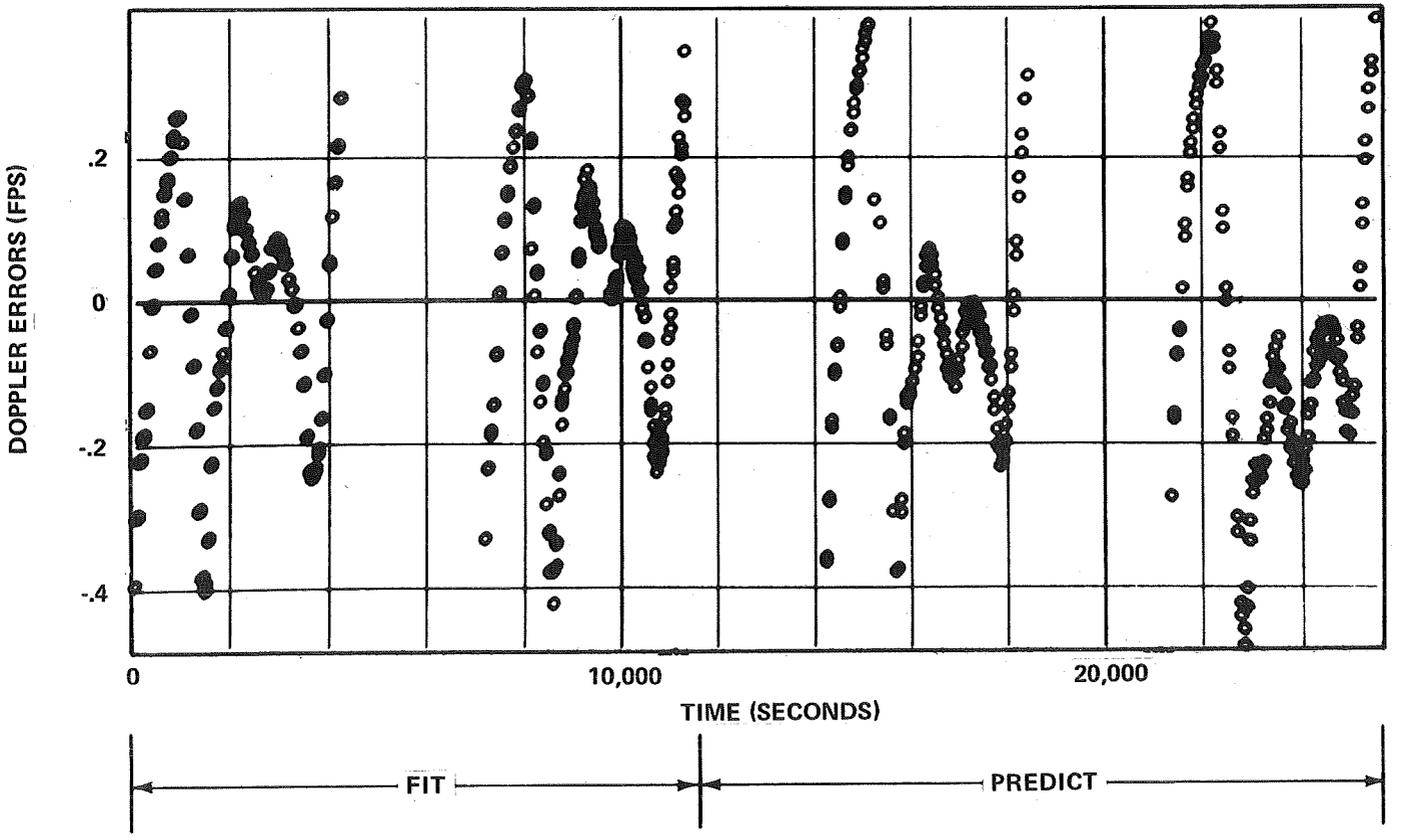
FIGURE 2 - DOPPLER RESIDUALS FROM TWO PASS SOLUTIONS AND
PREDICTIONS
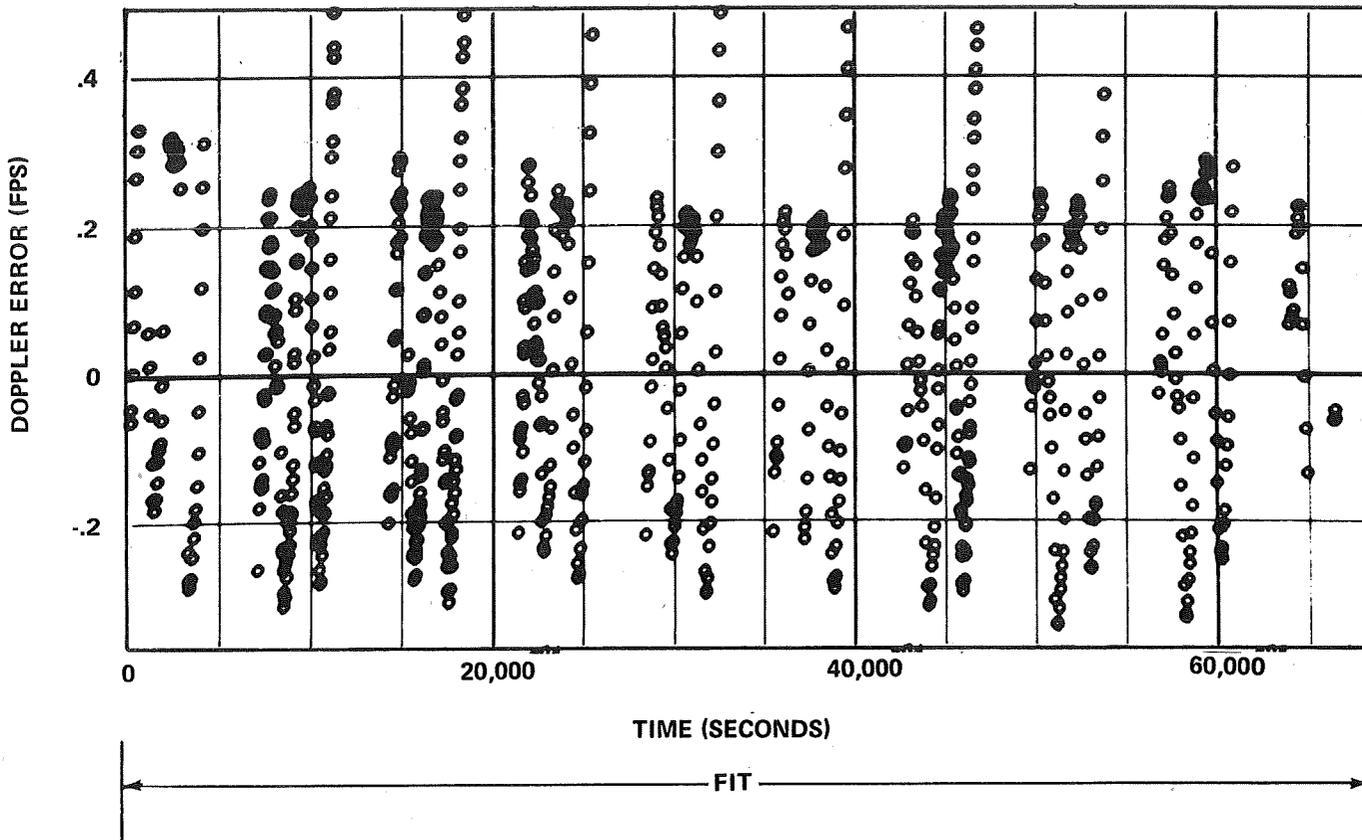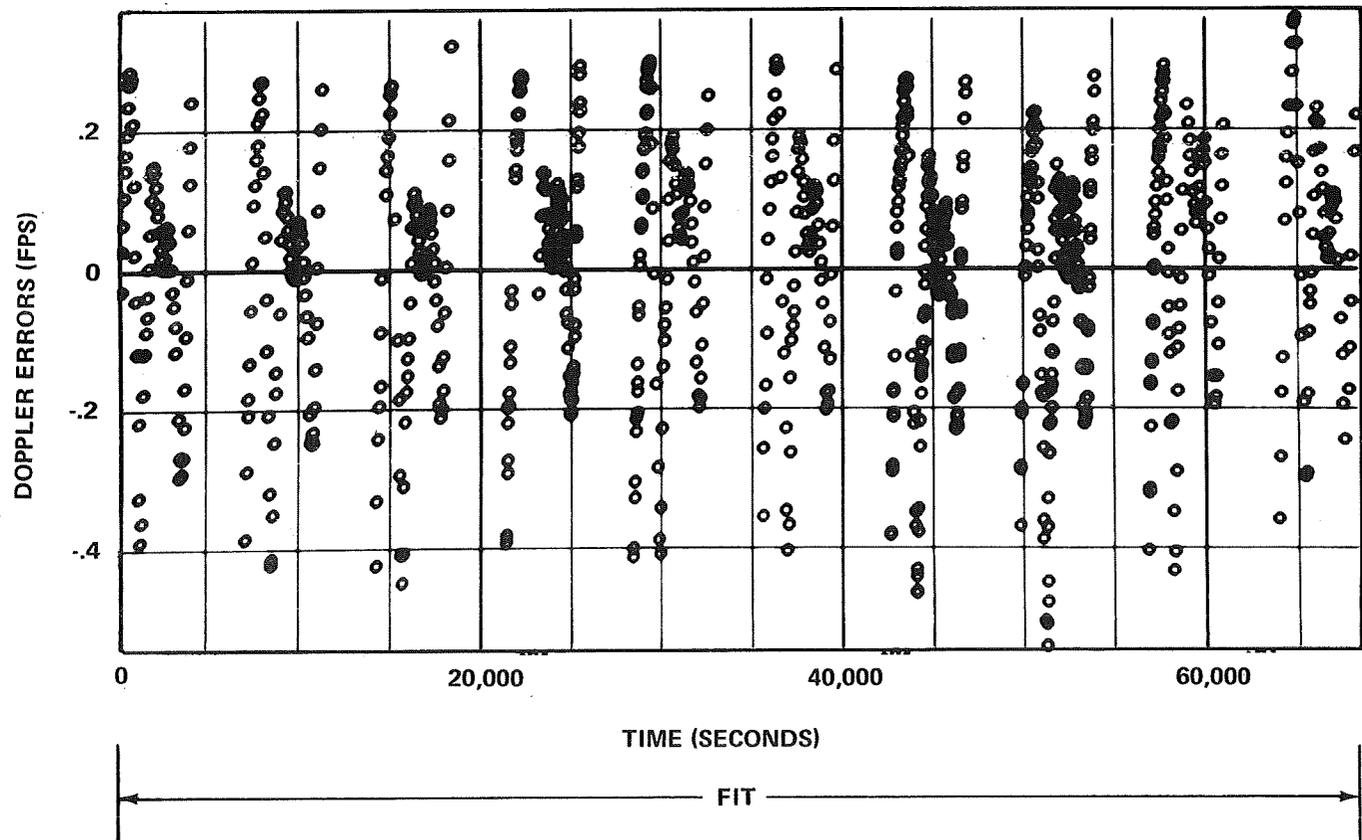
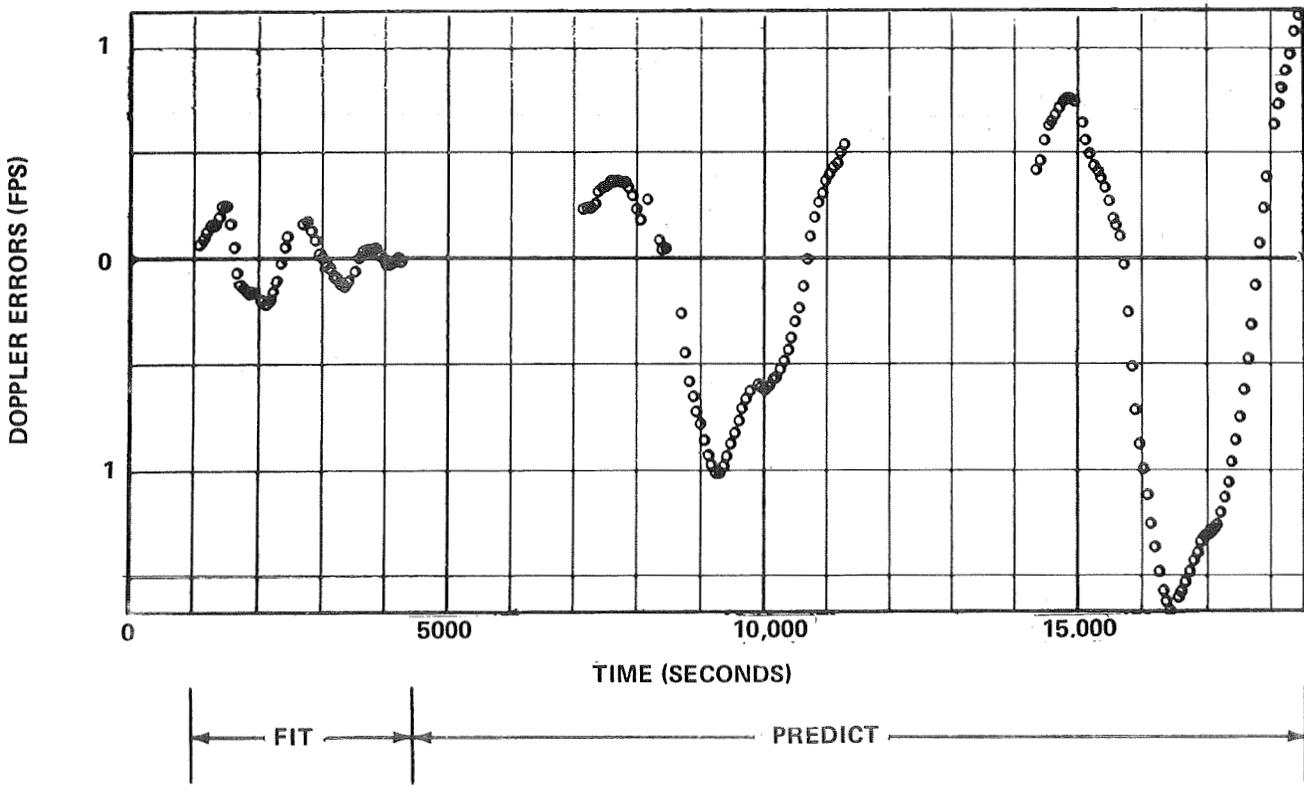FIGURE 3 - DOPPLER RESIDUALS FROM MULTI-PASS SOLUTIONS
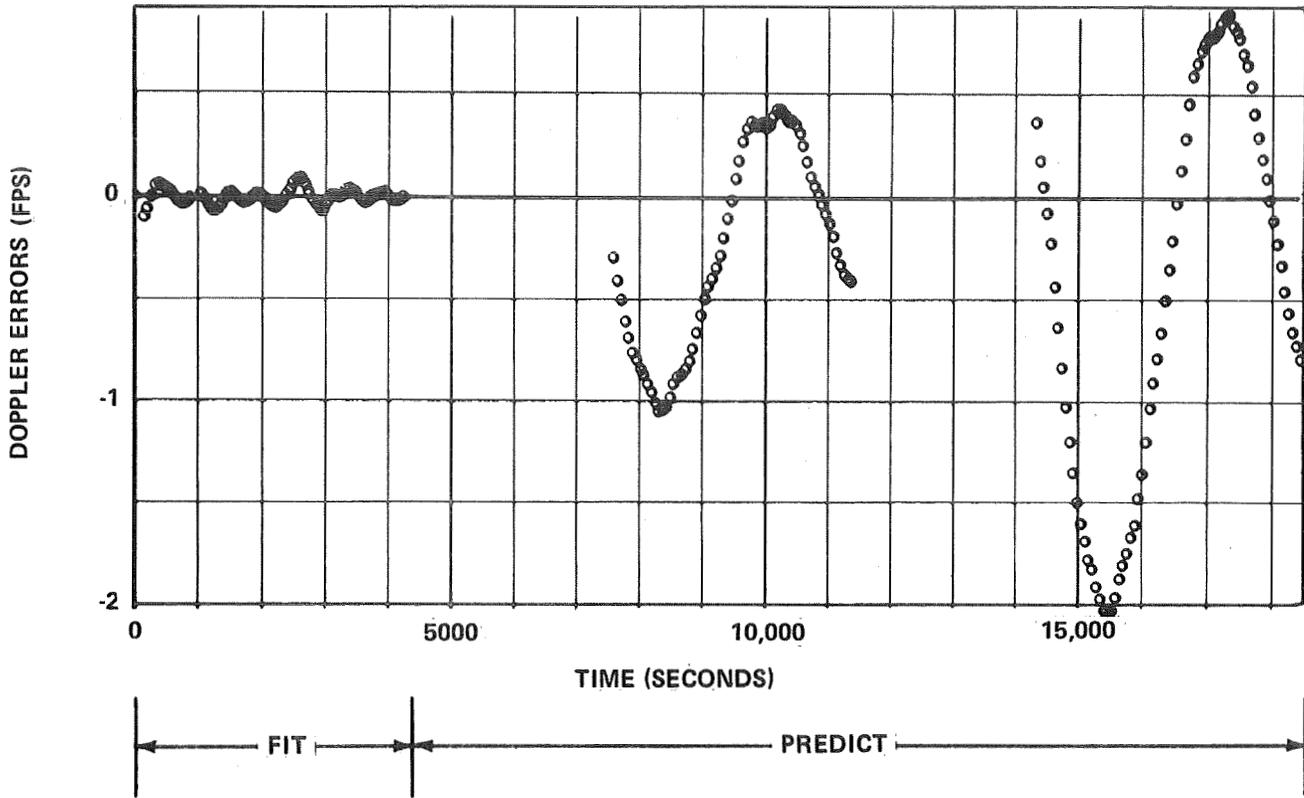
FIGURE 4 - DOPPLER RESIDUALS FROM ONE PASS SOLUTIONS
AND PREDICTIONS USING L1 GRAVITY FIELD

BELLCOMM, INC.

Subject: Orbit Determination for Lunar   From: M. V. Bullock
Parking Orbits Using Time-   A. J. Ferrari
Varying Orbital Elements

TR-70-310-2

DISTRIBUTION LIST

Complete Memorandum to

NASA Headquarters

J. K. Holcomb/MAO
T. A. Keegan/MA-2
C. M. King, Jr.,/MAT
C. M. Lee/MA
R. A. Petrone/MA
L. R. Scherer/MAL
W. C. Schneider/ML
J. B. Skaggs/MAP
G. C. White, Jr./MAR
NASA Headquarters Library (USS-10)

Goddard Space Flight Center

J. Barsky/554

Langley Research Center

S. G. Anderson/152A
W. T. Blackshear/152A
W. H. Michael, Jr./152A
R. H. Tolson/152A

Manned Spacecraft Center

M. Grogan/FM4
J. P. Mayer/FM
J. C. McPherson/FM4
E. Schiesser/FM4
W. Wollenhaupt/FM4

Bell Telephone Laboratories

W. M. Boyce/MH

Jet Propulsion Laboratory

P. Gottlieb/233-307
J. Lorell/156-217
P. Muller/198-112A
W. L. Sjogren/180-304

MIT/DL

R. H. Battin

Complete Memorandum to

Bellcomm, Inc.

D. R. Anselmo
A. P. Boysen, Jr.
J. O. Cappellari, Jr.
D. A. Corey
D. A. DeGraaf
W. W. Ennis
D. R. Hagner
W. G. Heffron
T. B. Hoekstra
D. B. James
M. G. Kelly
M. Liwshitz
D. D. Lloyd
K. E. Martersteck
W. I. McLaughlin
J. Z. Menard
B. G. Niedfeldt
D. H. Novak
G. T. Orrok
P. E. Reynolds
R. V. Sperry
C. C. H. Tang
W. B. Thompson
A. R. Vernon
J. E. Volonte
R. L. Wagner
All Members Department 2014
Department 1024 File
Central Files
Library

Abstract Only to

Bellcomm, Inc.

G. C. Bill
C. M. Harrison
B. T. Howard
I. M. Ross
C. M. Thomas
J. W. Timko
M. P. Wilson